

Deterministic coupling of quantum emitters in WSe₂ monolayers to plasmonic nanocavities

Oliver Iff,[†] Nils Lundt,[†] Simon Betzold,[†] Laxmi Narayan Tripathi,^{‡,†} Monika
Emmerling,[†] Young Jin Lee,[¶] Soon-Hong Kwon,[¶] Sven Höfling,^{†,§} and Christian
Schneider^{*,†}

[†]*Technische Physik and Wilhelm Conrad Röntgen Research Center for Complex Material
Systems, Physikalisches Institut, Universität Würzburg, Am Hubland, D-97074 Würzburg,
Germany*

[‡]*Department of Physics, Birla Institute of Technology, Mesra, Ranchi 835215, Jharkhand,
India*

[¶]*Department of physics, Chung-Ang University, Seoul, South Korea*

[§]*SUPA, School of Physics and Astronomy, University of St. Andrews, St. Andrews KY16
9SS, United Kingdom*

E-mail: christian.schneider@physik.uni-wuerzburg.de

Abstract

We discuss coupling of site-selectively induced quantum emitters in exfoliated mono-
layers of WSe₂ to plasmonic nanostructures. Squared and rectangular gold nanopillars,
which are arranged in pitches of 4 μm on the surface, have sizes of tens of nanometers,
and act as seeds for the formation of quantum emitters in the atomically thin materials.
We observe characteristic narrow-band emission signals from the monolayers, which
correspond well with the positions of the metallic nanopillars with and without thin

dielectric coating. Single photon emission from the emitters is confirmed by autocorrelation measurements, yielding $g^2(\tau = 0)$ values as low as 0.17. Moreover, we observe a strong co-polarization of our single photon emitters with the frequency matched plasmonic resonances, indicating deterministic light-matter coupling. Our work represents a significant step towards the scalable implementation of coupled quantum emitter-resonator systems for highly integrated quantum photonic and plasmonics applications.

Introduction

Creating solid state quantum emitters and their integration in micro- and nanophotonic structures is one of the prime tasks in modern quantum engineering. Coupled solid state quantum emitter-cavity systems range among the most promising candidates for the realization of highly efficient single photon sources,^{1–5} spin photon interfaces,^{6,7} quantum sensing probes⁸ as well as building blocks for quantum simulation⁹ and surface code quantum computing.¹⁰ While quantum emitters have been identified, studied and engineered in a variety of crystals including III-V¹¹ and II-VI quantum dots,^{12–14} colour defects in diamonds,¹⁵ impurities in SiC and organic polymers,^{16,17} atomically thin materials^{18–22} were recently established as a novel platform of quantum photonic devices. Quantum dots in III-V semiconductors and defect centers in diamonds certainly belong to the most mature implementations,²³ but the quality of site-controlled emitters leaves still needs to be improved, putting a serious thread regarding their scalable fabrication in ordered arrays.²⁴ Ordered InAs/GaAs quantum dot arrays have been realized by selective area growth methods and epitaxial growth on patterned substrates,²⁵ but in most cases the costly fabrication methods severely compromised their emission properties. Direct integration of positioned solid state quantum emitters with photonic resonators has been accomplished,^{26–28} but only in very selected cases and genuine scalability has remained elusive.

The formation of quantum emitters in mono- and bilayers of transition metal dichalcogenides has now been observed in various implementations: initially, localized luminescence

centers in exfoliated flakes were discovered close to their edges, and have been associated with strain wrinkles.^{20–22} In epitaxially grown flakes, random positioning of such spots was observed,¹⁸ indicating emission from defect bound excitons. Recently, the formation of quantum emitters on modulated metal substrates,^{29,30} as well as nanopillars^{31,32} was reported and associated with localized and engineered crystal strain fields, which outlines the unique possibility to deterministically induce quantum emitters in a straight forward manner by structuring the sample surface prior to the transfer.

While the ordered formation of quantum emitters thus far has been mainly observed on dielectric, nanostructured surfaces, spontaneous emission enhancement was reported on rough metallic surfaces and gold-coated nanopillars, giving rise to localized plasmonic modes.^{30,33} Combining atomically thin materials which comprise either tightly localized excitons or strongly bound free excitons with nanoplasmonic cavities yields a promising pathway to study light-matter coupling on the nanoscale enabled by the enormous field enhancements provided by metallic nanostructures.^{34,35} However, the deterministic coupling of well-ordered quantum emitters in atomically thin materials with resonant plasmonic modes has only now been achieved.^{33,36}

Sample Structure and Setup

In this work, we demonstrate the feasibility to induce ordered arrays of quantum emitters by defined arrays of metallic nanopillars, fabricated on a SiO₂ substrate. Such structures directly represent a coupled quantum dot-nanocavity system, and act as polarization-controlled single photon sources.

The sample consists of a semi-insulating silicon substrate, with a 200 nm thick SiO₂ layer on top. In order to fabricate the nanopillars, we first spin-coated a thin layer of PMMA and performed electron beam lithography to selectively expose rectangular areas in the resist with dimensions of 20 nm - 240 nm. After developing the resist, a 80 nm thick gold layer was

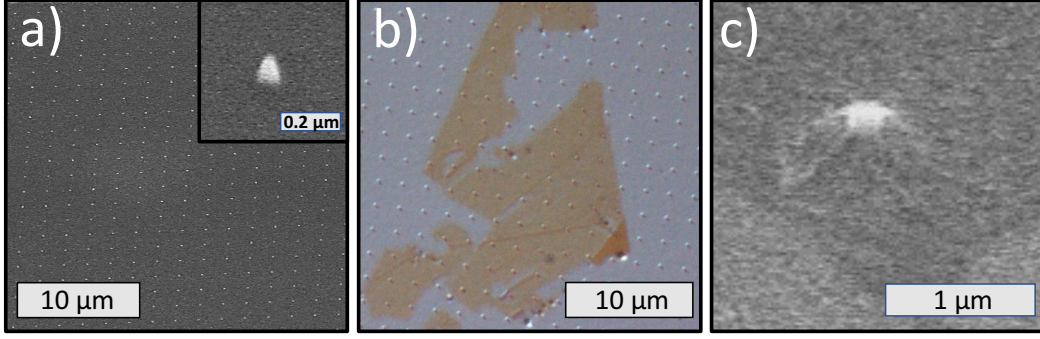


Figure 1: (a) Scanning electron microscope (SEM) image of the sample surface comprising metallic nanopillars as quantum emitter seeds and plasmonic nano-cavities. Inset: close-up view of a nanopillar. (b) Optical image of the pillar array after successful dry-transfer of an atomically thin WSe₂ monolayer. (c) Close-up SEM image of a single pillar covered by a strained monolayer, showing the formation of wrinkles.

evaporated on the sample, followed by a lift-off step. A scanning electron microscope (SEM) image of a prototype nanopillar array with a pitch of 2 μm is shown in Fig. 1a). On selected samples we additionally deposited a 3 nm thin layer of Al₂O₃ via atomic layer deposition. Next, we fabricated atomically thin layers of WSe₂ via mechanical exfoliation using adhesive tape, and transferred the layers on the pillar arrays via dry transfer³⁷ (Fig. 1b). We observe, that part of the pillars pierced the monolayer, while a substantial number of nanopillars (> 50 %) locally strained the layer, yielding the tent-like structure shown in Fig. 1c).

Spatially resolved optical spectroscopy was performed in a micro-photoluminescence setup with optional high spatial resolution (using fiber based confocal setting). The sample is excited by a frequency-doubled Nd:YAG laser at 532 nm, mounted in a liquid helium cooled flow cryostat.

Experimental Results and Discussion

Fig. 2a) depicts an exemplaric power dependent luminescence spectrum recorded on the position of a nanopillar with dielectric coating. The spectrum is widely dominated by a zoo of sharp emission lines, a typical signature of strongly localized emission centers in the crystal. In the low-power regime, these emission lines exhibit a slightly sub-linear intensity

increase with the pump power prior to their saturation level (Fig. 2b). This behaviour is mainly due to the gold pillars absorbing parts of the incident laser light,³⁸ but also the re-emitted light from the emitter, reducing their quantum efficiency.

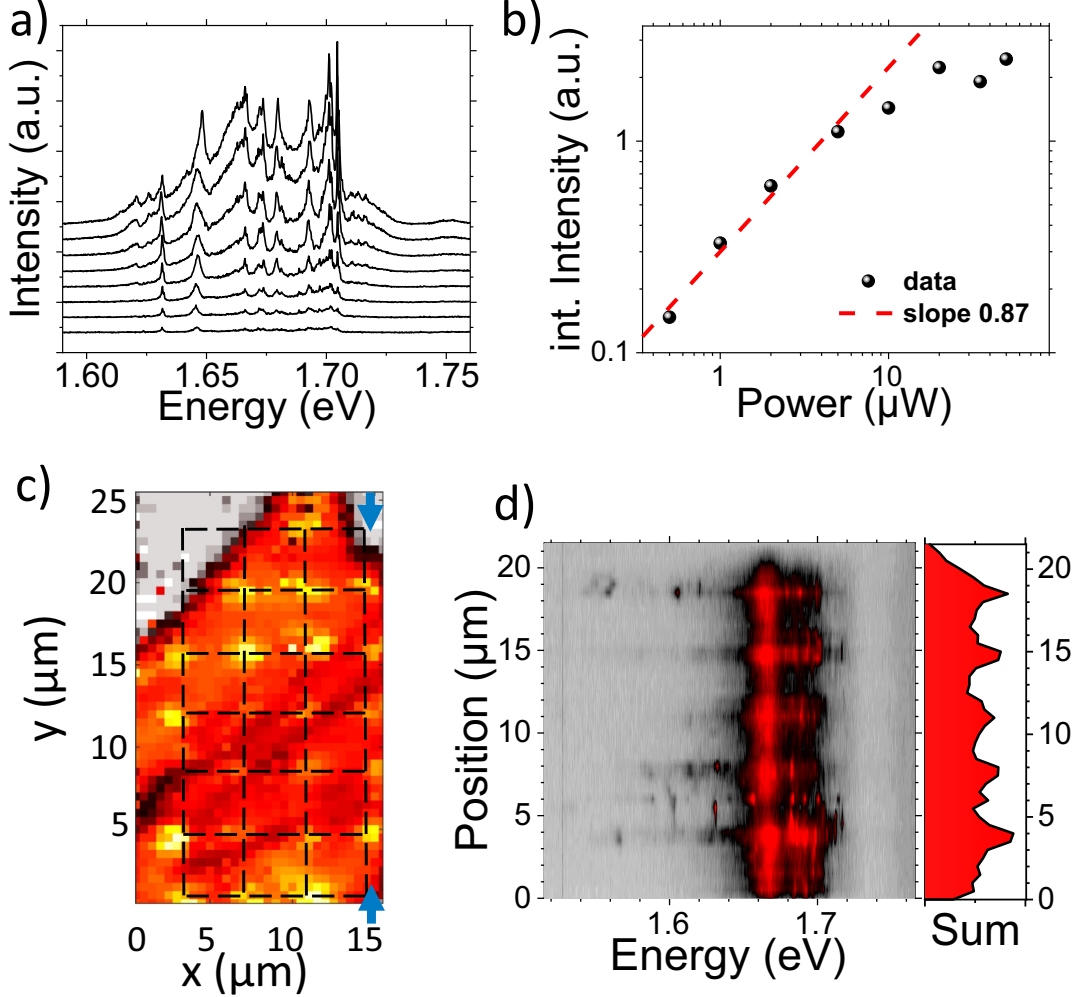


Figure 2: a) Power-dependent spectra on a nanopillar revealing many discrete emitters. b) Power-dependent study of a quantum emitter emission line before saturation starts above 10 μ W. c) Spatial map of a WSe₂ flake covering the nano-pillar array, showing the integrated intensity from 700 – 800 nm. The enhanced PL coincides with the 4 μ m pillar distance (black pattern). d) Spectral information extracted between the blue arrows in c), revealing a periodic increase in luminescence and the formation of additional localized emission centers.

The ordered formation of emitters on the nanopillar arrays is confirmed in a highly spatially resolved scanning microphotoluminescence study, applying the confocal configuration: Here, we carefully scan the sample's surface by utilizing a pair of motorized linear stages

with a step width of 500 nm underneath the excitation and collection spot. The spectrally integrated map (700-800 nm) is shown in Fig. 2c). It clearly evidences a regular pattern of bright emission sites, perfectly coinciding with the positions of the metallic pillars (dashed black pattern). Spectral information is best illustrated in a selected linescan between the blue arrows in Fig 2c). Here, we clearly observe a two-fold effect by the nanopillars (Fig. 2d): A strong luminescence enhancement of the overall signal due to plasmons,³⁹ as well as the regular formation of the sharp peaks below the free exciton energy (<1.74 eV), which we associate with tight exciton localization due to strain.

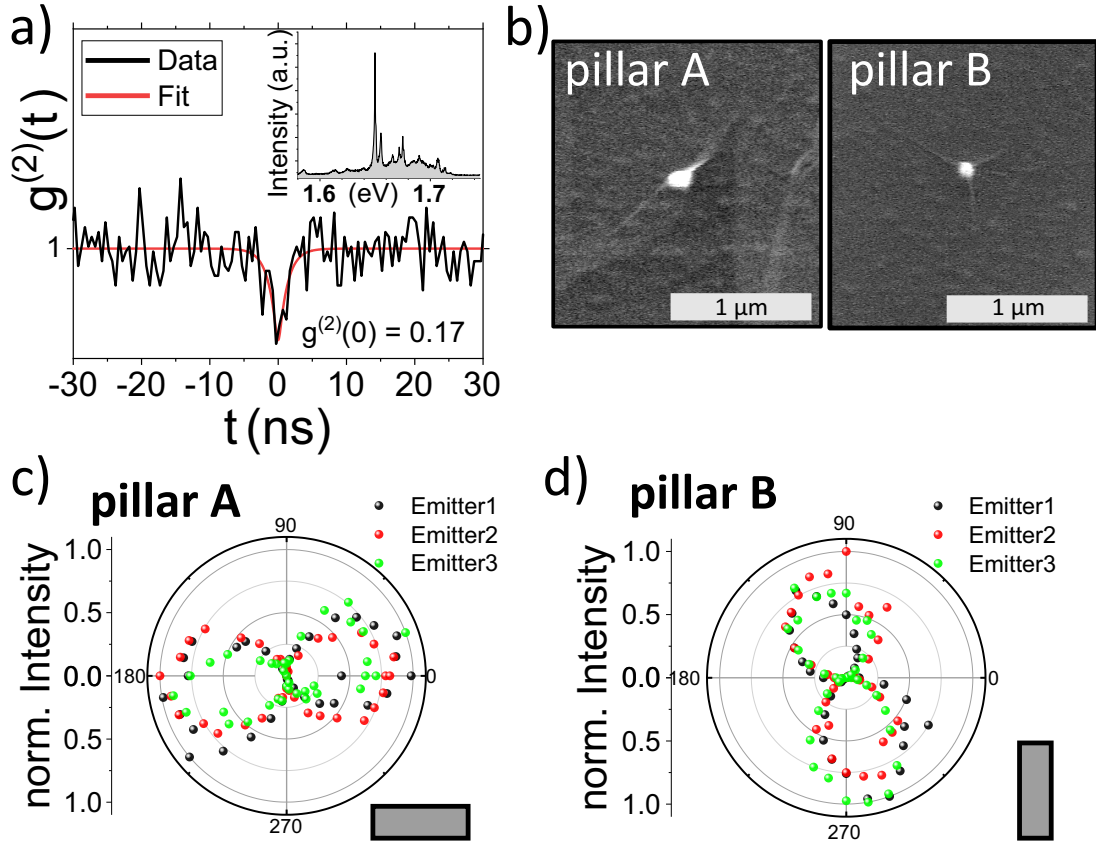


Figure 3: a) Second-order autocorrelation function of a quantum emitter on a pillar. The value of $g^{(2)}(\tau = 0) = 0.17$ confirms single photon emission. Inset: spectrum of single photon emitter. b) SEM images of two individual rectangles covered by WSe₂. Pillar A is horizontally and pillar B vertically aligned. c) and d) Polarization characteristic of three individual quantum emitters each on two different 90 nm \times 30 nm nanopillars shown in b).

In order to provide evidence for the capability to emit single photons from the deterministically localized excitons, we performed second order correlation measurements by exciting the sample with a 532 nm CW laser (Fig. 3a). We selected a dominant emission feature from one square pillar (140×140 nm). The luminescence was spectrally filtered (bandwidth: ≈ 300 μ eV, 300 grooves/mm grating) and passed to a fiber coupled Hanbury Brown and Twiss (HBT) setup. We observed a well-pronounced anti-bunching signal at zero delay time ($\tau = 0$), allowing us to extract a $g^{(2)}(\tau = 0)$ value of 0.17, which clearly puts our system in the regime of single photon emission.

Polarization resolved spectroscopy on different nanopillars revealed a strongly linear polarization of the luminescence from the emitters. In Fig. 3b two exemplary $90 \text{ nm} \times 30 \text{ nm}$ pillars are shown which are aligned perpendicular to each other and covered by the monolayer. Comparing the polarization of several emitters from these two pillars shows a strong correspondence of the polarization and pillar orientation (Fig. 3c,d). This alignment of the polarization along the long axis of the given gold rectangle can be associated with the coupling of the emitter to the plasmonic excitations in the metal which are much more pronounced in the extended axes as has been demonstrated with similar plasmonic structures before.⁴⁰ Slight modifications of the rotation angle also depends on the way the monolayer bends around the pillar, which further acts on the polarization of the emission.²⁹

Theory

In order to understand the optical enhancement of the quantum emitters in a WSe₂ via a metal nanopillar array, we investigated the plasmon modes excited in a square and a rod-like nanopillar by finite-difference time-domain (FDTD) method. In a square pillar with a size of $140 \text{ nm} \times 140 \text{ nm}$, the electric field distribution on top surface of the pillar is calculated, as shown in Fig. 4(a), where a quantum emitter of WSe₂ can be placed. At two vertical side edges orthogonal to the E_x polarization, strong field enhancement (E/E_0) with a maximum

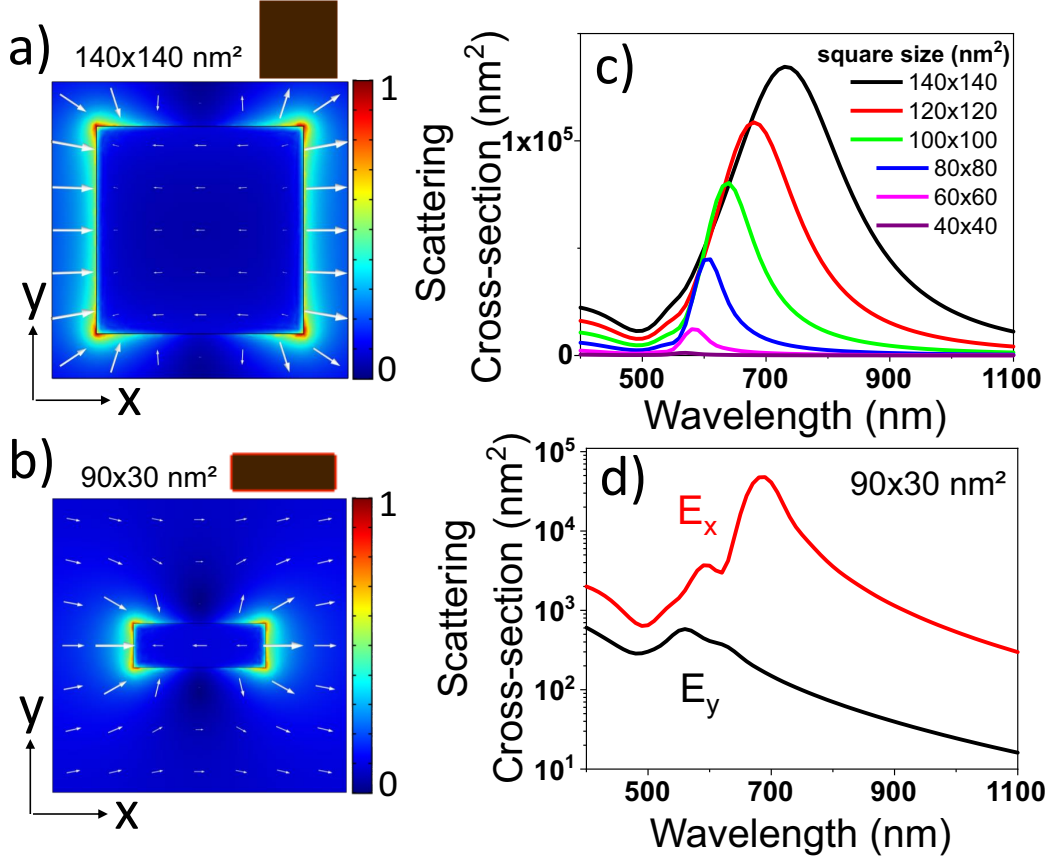


Figure 4: FDTD simulation: Vector maps of the field distribution and electric field enhancement E/E_0 at top surface of a pillar with a) a square cross-section of $(140 \text{ nm} \times 140 \text{ nm})$ and a rod-like cross-section of $(90 \text{ nm} \times 30 \text{ nm})$ excited by an electromagnetic field E_0 of 1 V/m at 740 nm . c) Calculated scattering cross-section spectrum of square nanopillars with different size from 140 nm to 40 nm . d) Two scattering cross-section spectra of a rod-like nanopillar with a size of $90 \text{ nm} \times 30 \text{ nm}$ for an incident light with orthogonal polarizations, E_x (red) and E_y (black). x-direction represents the direction of the long edge of the rod-like nanopillar.

value of 20 compared with an incident light is observed. In addition, vector plot shows the field enhancement is strongly attributed from the E_x field at the edges. Because an emitter in 2D materials oscillates in plane, strong emission enhancement for the defect emitters at the edges can be induced by the resonant coupling of the plasmon mode. The mode of the Fig. 4a is obtained by assuming E_x linearly polarized incident light, and a 90-degree rotated mode (not shown in the Figure) can also be observed for E_y polarized incident light. Scattering cross-section spectrum of Fig. 4(c) represents the spectral dependence of the plasmonic mode in a square pillar for different sizes of the side edges from 40 nm to 140 nm, where the resonant peak for a size of 140 nm \times 140 nm is 733 nm with a large FWHM of 234 nm. Therefore, the radiative emission of the quantum emitter with a spectrum of Fig. 3(a) can be enhanced by resonant coupling with a plasmonic mode. The plasmon resonance shifts blue with decreasing the size.

In order to understand the strong polarization dependence of the emission from a rod-like nanopillar, the mode profile and the scattering cross-section of a rod-like nanopillar with a cross-section of 90 nm \times 30 nm are investigated. For the E_x polarized incident light, the electric field distribution of the plasmonic mode in Fig. 4b is similar with that of a square pillar, Fig. 4a except for that the mode is elongated along the x-direction following the rod-like shape. In the scattering cross-section spectrum, the rod-like pillar exhibits strong plasmon resonance peak at a wavelength of 686 nm for an E_x polarized light, however, there are no significant resonances for an E_y polarized light. Therefore, 90 nm \times 30 nm nanopillar can enhance the x-directionally polarized emission of a quantum emitter and suppress the y-directionally polarized emission, resulting in strong linear polarization aligned along the long axis, as shown in Figs. 3(c) and (d).

Summary

In conclusion, we demonstrated the formation of ordered arrays of quantum emitters in an atomically thin layer of WSe₂, transferred on a metal nanopillar array. The gold nanopillars yield the formation of quantum emitters, and furthermore can act as plasmonic resonators granting active polarization control via deterministic light-matter coupling. Our work is a first step towards highly scalable cavity quantum electrodynamics with engineered quantum emitters in two dimensional materials.

Funding: State of Bavaria, H2020 European Research Council (ERC). National Research Foundation of Korea, Korean Government Grant NRF-2016R1C1B2007007.

References

- (1) Ding, X.; He, Y.; Duan, Z. C.; Gregersen, N.; Chen, M. C.; Unsleber, S.; Maier, S.; Schneider, C.; Kamp, M.; Höfling, S.; Lu, C. Y.; Pan, J. W. On-Demand Single Photons with High Extraction Efficiency and Near-Unity Indistinguishability from a Resonantly Driven Quantum Dot in a Micropillar. *Physical Review Letters* **2016**, *116*, 1–6.
- (2) Schlehahn, A.; Thoma, A.; Munnely, P.; Kamp, M.; Höfling, S.; Heindel, T.; Schneider, C.; Reitzenstein, S. An electrically driven cavity-enhanced source of indistinguishable photons with 61% overall efficiency. *APL Photonics* **2016**, *1*, 011301.
- (3) Unsleber, S.; He, Y.-M.; Maier, S.; Gerhardt, S.; Lu, C.-Y.; Pan, J.-W.; Kamp, M.; Schneider, C.; Höfling, S. Highly indistinguishable on-demand resonance fluorescence photons from a deterministic quantum dot micropillar device with 74 % extraction efficiency. *Opt. Express* **2015**, *24*, 1023–1030.
- (4) Senellart, P.; Solomon, G.; White, A. High-performance semiconductor quantum-dot single-photon sources. *Nature Nanotechnology* **2017**, *12*, 1026–1039.

- (5) Chang, W. H.; Chen, W. Y.; Chang, H. S.; Hsieh, T. P.; Chyi, J. I.; Hsu, T. M. Efficient single-photon sources based on low-density quantum dots in photonic-crystal nanocavities. *Physical Review Letters* **2006**, *96*, 3–6.
- (6) De Greve, K.; Yu, L.; McMahon, P. L.; Pelc, J. S.; Natarajan, C. M.; Kim, N. Y.; Abe, E.; Maier, S.; Schneider, C.; Kamp, M.; Höfling, S.; Hadfield, R. H.; Forchel, A.; Fejer, M. M.; Yamamoto, Y. Quantum-dot spin-photon entanglement via frequency downconversion to telecom wavelength. *Nature* **2012**, *491*, 421–425.
- (7) Gao, W. B.; Fallahi, P.; Togan, E.; Miguel-Sanchez, J.; Imamoglu, A. Observation of entanglement between a quantum dot spin and a single photon. *Nature* **2012**, *491*, 426–430.
- (8) Anker, J. N.; Hall, W. P.; Lyandres, O.; Shah, N. C.; Zhao, J.; Van Duyne, R. P. Biosensing with plasmonic nanosensors. *Nature Materials* **2008**, *7*, 442–453.
- (9) Wang, H. et al. High-efficiency multiphoton boson sampling. *Nature Photonics* **2017**, *11*, 361.
- (10) Greve, K. D.; Press, D.; McMahon, P. L.; Yamamoto, Y. Ultrafast optical control of individual quantum dot spin qubits. *Reports on Progress in Physics* **2013**, *76*.
- (11) Michler, P.; Imamoglu, A.; Mason, M. D.; Carson, P. J.; Strouse, G. F.; Buratto, S. K. Quantum correlation among photons from a single quantum dot at room temperature. *Nature* **2000**, *406*, 968–970.
- (12) Peng, X.; Manna, L.; Yang, W.; Wickham, J.; Scher, E.; Kadavanich, A.; Alivisatos, A. P. Shape control of CdSe nanocrystals. *Nature* **2000**, *404*, 59–61.
- (13) Lowisch, M.; Rabe, M.; Stegemann, B.; Henneberger, F.; Grundmann, M.; Türec, V.; Bimberg, D. Zero-dimensional excitons in (Zn,Cd)Se quantum structures. *Physical review. B, Condensed matter* **1996**, *54*, R11074–R11077.

- (14) Xin, S. H.; Wang, P. D.; Yin, A.; Kim, C.; Dobrowolska, M.; Merz, J. L.; Furdyna, J. K. Formation of self-assembling CdSe quantum dots on ZnSe by molecular beam epitaxy. *Applied Physics Letters* **1996**, *69*, 3884–3886.
- (15) Kurtsiefer, C.; Mayer, S.; Zarda, P.; Weinfurter, H. Stable solid-state source of single photons. *Physical Review Letters* **2000**, *85*, 290–293.
- (16) Castelletto, S.; Johnson, B. C.; Ivády, V.; Stavrias, N.; Umeda, T.; Gali, A.; Ohshima, T. HL 113 : Quantum information systems II (with TT). *Nature Materials* **2013**, *12*, 1–6.
- (17) Castelletto, S.; Johnson, B. C.; Zachreson, C.; Beke, D.; Balogh, I.; Ohshima, T.; Aharonovich, I.; Gali, A. Room temperature quantum emission from cubic silicon carbide nanoparticles. *ACS Nano* **2014**, *8*, 7938–7947.
- (18) He, Y.-M.; Clark, G.; Schaibley, J. R.; He, Y.; Chen, M.-C.; Wei, Y.-J.; Ding, X.; Zhang, Q.; Yao, W.; Xu, X.; Lu, C.-Y.; Pan, J.-W. Single quantum emitters in monolayer semiconductors. *Nature Nanotechnology* **2015**, *10*, 497–502.
- (19) Srivastava, A.; Sidler, M.; Allain, A. V.; Lembke, D. S.; Kis, A.; Imamoglu, A. Optically active quantum dots in monolayer WSe₂. *Nature Nanotechnology* **2015**, *10*, 491–496.
- (20) Tonndorf, P.; Schmidt, R.; Schneider, R.; Kern, J.; Buscema, M.; Steele, G. a.; Castellanos-Gomez, A.; van der Zant, H. S. J.; Michaelis de Vasconcellos, S.; Bratschkitsch, R. Single-photon emission from localized excitons in an atomically thin semiconductor. *Optica* **2015**, *2*, 347.
- (21) Koperski, M.; Nogajewski, K.; Arora, A.; Cherkez, V.; Mallet, P.; Veuillen, J.-Y.; Marcus, J.; Kossacki, P.; Potemski, M. Single photon emitters in exfoliated WSe₂ structures. *Nature Nanotechnology* **2015**, *10*, 503–506.

- (22) Kumar, S.; Kaczmarczyk, A.; Gerardot, B. D. Strain-Induced Spatial and Spectral Isolation of Quantum Emitters in Mono- and Bilayer WSe₂. *Nano Letters* **2015**, *15*, 7567–7573.
- (23) Balasubramanian, G.; Chan, I. Y.; Kolesov, R.; Al-Hmoud, M.; Tisler, J.; Shin, C.; Kim, C.; Wojcik, A.; Hemmer, P. R.; Krueger, A.; Hanke, T.; Leitenstorfer, A.; Bratschitsch, R.; Jelezko, F.; Wrachtrup, J. Nanoscale imaging magnetometry with diamond spins under ambient conditions. *Nature* **2008**, *455*, 648–651.
- (24) Van Der Sar, T.; Heeres, E. C.; Dmochowski, G. M.; De Lange, G.; Robledo, L.; Oosterkamp, T. H.; Hanson, R. Nanopositioning of a diamond nanocrystal containing a single nitrogen-vacancy defect center. *Applied Physics Letters* **2009**, *94*, 92–95.
- (25) Schmidt, O. G. *Lateral alignment of epitaxial quantum dots*; Springer Science & Business Media, 2007.
- (26) Gallo, P.; Felici, M.; Dwir, B.; Atlasov, K.; Karlsson, K. F.; Rudra, A.; Mohan, A.; Biasiol, G.; Sorba, L.; Kapon, E. Integration of site-controlled pyramidal quantum dots and photonic crystal membrane cavities. *Applied Physics Letters* **2008**, *263101*, 1–4.
- (27) Schneider, C.; Heindel, T.; Huggenberger, A.; Weinmann, P.; Kistner, C.; Kamp, M.; Reitzenstein, S.; Höfling, S.; Forchel, A. Single photon emission from a site-controlled quantum dot-micropillar cavity system. *Applied Physics Letters* **2009**, *94*, 1–4.
- (28) Sünner, T.; Schneider, C.; Strauss, M.; Huggenberger, A.; Wiener, D.; Höfling, S.; Kamp, M.; Forchel, A. Scalable fabrication of optical resonators with embedded site-controlled quantum dots. *Optics letters* **2008**, *33*, 1759–1761.
- (29) Kern, J.; Trügler, A.; Niehues, I.; Ewering, J.; Schmidt, R.; Schneider, R.; Najmaei, S.; George, A.; Zhang, J.; Lou, J.; Hohenester, U.; Michaelis De Vasconcellos, S.; Bratschitsch, R. Nanoantenna-Enhanced Light-Matter Interaction in Atomically Thin WS₂. *ACS Photonics* **2015**, *2*, 1260–1265.

- (30) Tripathi, L. N.; Iff, O.; Betzold, S.; Emmerling, M.; Moon, K.; Lee, Y. J.; Kwon, S.-H.; Höfling, S.; Schneider, C. Spontaneous emission enhancement in strain-induced WSe₂ monolayer based quantum light sources on metallic surfaces. *ACS Photonics* **2018**, *5*, 1919–1926.
- (31) Palacios-Berraquero, C.; Kara, D. M.; Montblanch, A. R.; Barbone, M.; Latawiec, P.; Yoon, D.; Ott, A. K.; Loncar, M.; Ferrari, A. C.; Atatüre, M. Large-scale quantum-emitter arrays in atomically thin semiconductors. *Nature Communications* **2017**, *8*, 1–6.
- (32) Branny, A.; Kumar, S.; Proux, R.; Gerardot, B. D. Deterministic strain-induced arrays of quantum emitters in a two-dimensional semiconductor. *Nature Communications* **2017**, *8*, 1–7.
- (33) Cai, T.; Kim, J.-h.; Yang, Z.; Dutta, S.; Aghaeimeibodi, S.; Waks, E. Radiative enhancement of single quantum emitters in WSe₂ monolayers using site-controlled metallic nano-pillars. **2018**, 1–20.
- (34) Krasnok, A.; Lepeshov, S.; Alú, A. Nanophotonics with 2D Transition Metal Dichalcogenides. *ArXiv* **2018**, *1801.00698*.
- (35) Lalanne, P.; Yan, W.; Vynck, K.; Sauvan, C.; Hugonin, J.-P. Light Interaction with Photonic and Plasmonic Resonances. *Laser & Photonics Reviews* **2018**, *1700113*, 1700113.
- (36) Luo, Y.; Shepard, G. D.; Ardelean, J. V.; Hone, J. C.; Strauf, S. Deterministic coupling of site-controlled quantum emitters in monolayer semiconductors to plasmonic nanocavities. *arXiv Mesoscale and Nanoscale Physics* **2018**, *1050*.
- (37) Castellanos-Gomez, A.; Buscema, M.; Molenaar, R.; Singh, V.; Janssen, L.; van der Zant, H. S. J.; Steele, G. a. Deterministic transfer of two-dimensional materials by all-dry viscoelastic stamping. *2D Materials* **2014**, *1*, 011002.

- (38) Link, S.; Mohamed, M. B.; El-Sayed, M. A. Simulation of the Optical Absorption Spectra of Gold Nanorods as a Function of Their Aspect Ratio and the Effect of the Medium Dielectric Constant. *The Journal of Physical Chemistry B* **1999**, *103*, 3073–3077.
- (39) Hugall, J. T.; Singh, A.; Van Hulst, N. F. Plasmonic Cavity Coupling. *ACS Photonics* **2018**, *5*, 43–53.
- (40) Luo, Y.; Ahmadi, E. D.; Shayan, K.; Ma, Y.; Mistry, K. S.; Zhang, C.; Hone, J.; Blackburn, J. L.; Strauf, S. Purcell-enhanced quantum yield from carbon nanotube excitons coupled to plasmonic nanocavities. *Nature Communications* **2017**, *8*.